RESEARCH ARTICLE

BON VIEW PUBLISHING

Mathematical Analysis on Dispersion Relation of Rayleigh Wave for an Initially Stressed Magneto-Poroelastic Material with Corrugated and Impedance Boundary

Augustine Igwebuike Anya[1,*] , Ugochukwu David Uche[2] and Christian Nwachioma[3]

[1]GST-Mathematics Division, Veritas University Abuja, Nigeria

[2]Department of Mathematics, University of Abuja, Nigeria

[3]Department of Mechanical Engineering, University of Colorado Denver, USA

Abstract: This study showcases the Mathematical modeling of elastic surface waves and the analysis of dispersion relations of Rayleigh type of wave in an initially stressed homogeneous porous magneto-elastic material having corrugated and impedance boundary exhibitions. Adoption of the classical harmonic method of wave analysis, non-dimensionalization of the resulting equations of motion, and corrugated-impedance boundary conditions produced by the modeled problem are also captured. The dispersion equation was analytically and graphically presented. Effects of the contributing physical quantities, such as impedance and corrugated boundary parameters, on Rayleigh waves for the chosen material are analyzed. The magnetic field's influences and the wavenumber associated with the corrugated boundary surfaces on the material increase the dispersion relations of the Rayleigh wave profile on the material. In addition, we noted that the dispersion relations of the wave increase for increasing phase velocity and some parameters of voids. Also, a void parameter triggered a decrease on the dispersion profile of the Rayleigh wave when increased while noting some uniform exhibitions from other void coefficients. This work holds the potential to provide more insights into studies involving displacement distributions in earthquake sciences, stress-strain analysis in Structural Engineering materials, among others.

Keywords: Rayleigh wave, dispersion relation, void source, magnetic fields, mechanical force, initial stress, corrugation and impedance

1. Introduction

Dispersion relations of Rayleigh wave relate the wavelength or wavenumber of the wave to its frequency through which the phase velocity of waves in a material could be calculated. Rayleigh waves and Love waves are some typical examples of surface waves which are guided by the free surface of the earth. They come after P-wave and Sv-wave had gone through the body of a material and usually involves horizontal particle motion. Thus, the examination of disturbances which occurs naturally (for instance; earthquakes) and artificially, in solid mechanics, is still much in vogue; based on insights from models that describe these occurrences. Civil engineering, geophysics and geotechnical, Mathematics of waves, etc., are important areas of specializations where the knowledge of these models on materials or structures is paramount. Spencer [1] studied known composite materials like the fiber-reinforced composites and depicted its light weight and stiffness characteristics which have endeared them to some wide range of applications in areas such as the fields of engineering and architectural designs. Despite this, some given physical properties and parameters such as initially stressed material like the earth [2], magnetic fields, etc., are sometimes incorporated in the material makeup [3], to make sense of behaviors linked with materials that are subjected to disturbances especially on surfaces where elastic surface waves like the Rayleigh-type wave could propagate. Also opined by similar view is Cowin and Nunziato [4], whose works dealt on volume fraction fields as a useful generalization to mechanical characteristics of materials. Voids or pores on materials have no dimension in material sciences. It unarguably results from poor manufacturing processes which oftentimes are deemed undesirable to the mechanical and lifespan attributes of materials. Although, it has wide range of applications in mechanical and aerospace engineering, and most especially as it inculcates the degree of freedom and sensitivity of the applications to the composites.

Furthermore, boundary surfaces of some materials are entirely of different geometry in nature, for example, the grooved boundary surface. This grooved shape could be seen as a series of parallel furrows and ridges on materials [5]. Also, observing from a 3D point of view, a corrugated metallic media is an anisotropic boundary surface. And the surface waves excited on any metallic corrugated surface possess a phase velocity which is dependent on

*Corresponding author: Augustine Igwebuike Anya, GST-Mathematics Division, Veritas University Abujaa, Nigeria. Email: anyaa@veritas.edu.ng

the propagation direction and so many other characterizations of plane waves in a 2D anisotropic material configuration. Usually, most surface wave fronts produced by a point source close to a corrugated metallic boundary yields complicated curves as compared with that produced by elliptical wave front of a point source in 2D anisotropic martial configurations. Corrugation is seen as an age long means of obtaining lightweight material media embedded with considerably high anisotropic behaviors and stability under load buckling. In modern times, advanced, ingenious, and innovative corrugated geometries are being sought after, for example, the morphing media which tend to seek the full use of the extreme anisotropy of grooved sheets, by adopting flexible degrees of freedom. Thus, all these could contribute and attest to the causations of dispersions relations and in hitherto the geometric boundary conditions or by wave's interaction with the transmitting medium. Hence, it suffices to add that when dispersion relation occurs on material media, a wave does not move with an unchanging waveform. This undoubtedly will produce distinct frequencies. It is to be noted that matter waves, even in the absence of these geometric conditions, possess a non-trivial dispersion relation. Be that as it may, impedance boundary conditions are a linear combination of unknown functions and their derivatives prescribed on the boundary [6]. While impedance on the other hand is a measure of the opposition that a system possesses to the acoustic flux due to an acoustic pressure applied to the media. This type of boundary conditions may provide some relevant applications where a given electromagnetic field penetrates only at short coverage outside the given boundary and in turn providing an approximation to this penetration to avoid including another form of domain in the modeled problem. These are often utilized in various fields such as in electro-magneto-acoustics occurrences like the electromagnetic acoustic imaging in some biomedical appliances, etc.,

2. Literature Review

Consequently, some authors have made contributions to this concepts of impedance and corrugated boundaries and other related wave propagation phenomena [7–22], as an individual or part considerations of the interacting physical quantities rather than in combined effect as presented in this investigation. Also, Zghal et al. [23] dealt on free vibration analysis of porous beams with gradually varying mechanical properties. Also, Kundu et al. [24] contributed to field by investigating the effect of initial stress on the propagation and attenuation characteristics of Rayleigh waves on a media. Moreover, Singh et al. [20] worked on dispersion of love waves while considering Influence of corrugated boundary surfaces, reinforcement, hydrostatic stress, heterogeneity, and anisotropy of the material without porosity and impedance characterizations on Rayleigh type of waves.

Subsequently, the current investigation is centered on deriving a Mathematical model that would account for the analysis of surface waves and in particular the dispersion of Rayleigh waves in porous magneto-elastic material. The equations of motion are analytically presented after the formulations of the model with the characterized physical quantities of initial stress, magnetic influences, corrugation, and impedance. Owing to these combined physical quantities incorporated in the model, some comparable degrees of uniqueness and innovations are achieved. The normal

mode analysis utilized in solving the problem is well suited as a usual classical approach for wave analysis in continuum mechanics of materials. Computational solutions for the effects of these physical quantities on the dispersion relations of the Rayleigh wave were equally depicted using Mathematica Software for a particular chosen material. Thus, this study also points to the fact that the nature of surfaces of materials with corrugation must have negligible initial stress for the occurrence of a mathematical dynamic response of dispersion relation of Rayleigh-type wave.

3. The Mathematical Model and Formulations

The constitutive equations for an initially stressed porous fiber-reinforced composite with magnetic influence Biot [2], Spencer [1], Othman et al. [26], Abd-Alla et al. [3], and Anya et al. [9] are specified by:

$$\alpha_{ij} = -P(\delta_{ij} + \varpi_{ij}) + \lambda\varepsilon_{kk}\delta_{ij} + 2\mu_T\varepsilon_{ij} \quad + \alpha(s_k s_m \varepsilon_{km}\delta_{ij} + \varepsilon_{kk}s_i s_j)$$
$$+ 2(\mu_L - \mu_T) \quad (s_i s_k \varepsilon_{kj} + s_j s_k \varepsilon_{ki}) + \beta(s_k s_m \varepsilon_{km}s_i s_j) + \xi\delta_{ij}\phi, \tag{1}$$

$$F_i = \mu_0 H_0^2 \left(e_{,1} - \varepsilon_0\,\mu_0\ddot{u}_1,\, e_{,2} - \varepsilon_0\,\mu_0\ddot{u}_2,\, 0\right), \tag{2}$$

α_{ij} represents the stress tensor, ε_{ij} is the strain tensor, δ_{ij} is the Kronecker delta function, λ is Lames constant, $(\alpha, \beta, (\mu_L - \mu_T))$ are the fiber-reinforced parameters, u_i displacement components, ϕ is the volume fraction fields, P is the initially stressed parameter, ϖ_{ij} is the rigid body rotation also called spin tensor and F_i is the magnetic force $i = j = 1, 2, 3$. Also, $e = (u_{1,1} + u_{2,2})\ \varpi_{ij} = \frac{1}{2}(u_{i,j} - u_{j,i})$ and $\varepsilon_{ij} = \frac{1}{2}(u_{i,j} + u_{j,i})$. We consider $H_i = H_0\delta_{i3} + h_i$, such that h_i is the induced magnetic field; $h_i(x_1, x_2, x_3) = -u_{k,k}\delta_{i3}$. ε_o is electric permeability such that the solid medium lies in the $x_1 x_2 -$ plane. H_i is the magnetic vector field while μ_o is the magnetic permeability as adapted from Maxwell's equations of electromagnetism. Considerations were made such that $s = (s_1, s_2, s_3)$ stipulates the fiber directions and assumes the values $s = (1, 0, 0)$. Thus, in the presence of magnetic influences and porosity, the fields' equations take the forms:

$$\alpha_{ij,j} + F_i = \rho\ddot{u}_i, \tag{3}$$

$$\xi_1(\phi_{,ii}) - \omega_o\phi - \varpi\dot{\phi} - \xi(u_{i,i}) = \rho\kappa\ddot{\phi}. \tag{4}$$

Owing to the above formulations, we hinge our investigation in the $x_1 x_2-$ plane. This entails that $x_3 = 0$ and $x_1 \neq x_2 \neq 0$, whereas the displacements $u_1 \neq u_2 \neq u_3 \neq 0$. u_3 are uncoupled whereas $u_1 \neq u_2 \neq 0$ are coupled. Hence, the component forms of Equations (3–4) are given below:

$$B_1 u_{1,11} + B_2 u_{2,21} + B_3 u_{1,22} = \{\rho + \varepsilon_0\mu_0^2 H_0^2\}\ddot{u}_1 - \xi\phi_{,1}, \tag{5}$$

$$B_2 u_{1,12} + B_4 u_{2,11} + B_5 u_{2,22} = \{\rho + \varepsilon_0\mu_0^2 H_0^2\}\ddot{u}_2 - \xi\phi_{,2}, \tag{6}$$

$$\xi_1(\phi_{,ii}) - \omega_o\phi - \varpi\dot{\phi} - \xi(u_{i,i}) = \rho\kappa\ddot{\phi}. \tag{7}$$

$B_1 = (\lambda + 2\alpha + 4\mu_L - 2\mu_T + \beta + \mu_0 H_0^2)$,
$B_2 = (\alpha + \lambda + \mu_L + \mu_0 H_0^2 + P/2)$,
$B_3 = \mu_L - P/2, B_4 = \mu_L - P/2, B_5 = (\lambda + 2\mu_T + \mu_0 H_0^2)$.

We introduce the following dimensionless constants as a convenience to the above equations of motion; $(t') = c_0^2 t$, $\phi' = \phi$, $(x_1', x_2', u_1', u_2') = c_0(x_1, x_2, u_1, u_2)$ $\tau_{ij}' = \tau_{ij}/\rho c_0^2$, $c_0^2 = A_1/\rho$, into Equations (5–7). If the sign "'" is removed, Equations (5–7) results to:

$$u_{1,11} + B_{12}u_{2,21} + B_{13}u_{1,22} + B_{11}\phi_{,1} = \{1 + \varepsilon_0\mu_0^2 H_0^2/\rho\}\ddot{u}_1, \quad (8)$$

$$B_{12}u_{1,12} + B_{14}u_{2,11} + B_{15}u_{2,22} + B_{11}\phi_{,2} = \{1 + \varepsilon_0\mu_0^2 H_0^2/\rho\}\ddot{u}_2, \quad (9)$$

$$B_6(\phi_{,ii}) - B_7\phi - B_8\dot{\phi} - B_9(u_{,i}) = B_{10}\ddot{\phi}. \quad (10)$$

$$(B_{12}, B_{13}, B_{14}, B_{15}, B_6, B_8, B_{11}) = (B_2, B_3, B_4, B_5, \xi_1, \varpi, \xi)/B_1,$$
$$(B_7, B_9) = (\omega_o\rho, \xi\rho)/B_1^2, B_{10} = \kappa.$$

4. Analytical Solution

In this section, we make considerations such that the normal mode analysis or harmonic wave approach be adopted for the impedance and grooved boundary of the initially stressed fiber-reinforced solid in the half-space with porosity under magnetic fields. Owing to this, the wave displacements are considered as;

$$(u_j, \phi) = \{\bar{u}_j(x_2), \bar{\phi}(x_2)\}e^{\omega t + ibx_1}, j = 1, 2. \quad (11)$$

Substituting Equation (11) into Equations (8–10) yields the equations below:

$$(B_{13}D^2 - b^2 - (1 + \varepsilon_0\mu_0^2 H_0^2/\rho)\omega^2)\bar{u}_1 + (iB_{12}bD)\bar{u}_2 + bB_{11}i\bar{\phi} = 0, \quad (12)$$

$$(iB_{12}bD)\bar{u}_1 + (B_{15}D^2 - B_{14}b^2 - (1 + \varepsilon_0\mu_0^2 H_0^2/\rho)\omega^2)\bar{u}_2 + DB_{11}\bar{\phi} = 0, \quad (13)$$

$$-B_9ib\bar{u}_1 - B_9D\bar{u}_2 + (B_6D^2 - (B_6b^2 + B_7 + B_8\omega - B_{10}\omega^2))\bar{\phi} = 0. \quad (14)$$

A non-trivial solution of Equations (12–14) yields:

$$(G_1D^6 + G_2D^4 + G_3D^2 + G_4)(\bar{u}_1, \bar{u}_2, \bar{\phi}) = 0 \quad (15)$$

$G_i, i = 1, 2, 3, 4$ (See Appendix) represents complex coefficients which possess characteristics of the physical constants of the given material. Given that $v_i, i = 1, 2, 3$ gives positive real roots of the Equation (15), normal mode wave method prescribe the following form of solutions;

$$(\bar{u}_1, \bar{u}_2, \bar{\phi}) = \sum_{n=1}^{3}(M_n, M_{1n}, M_{2n})e^{-v_n x_2} \quad (16)$$

M_n, M_{1n} and M_{2n} are functions of the wave number b in the direction x_1 and the complex frequency ω of the waves. Putting Equation (16) into Equations (12–14), the relations are thus given;

$$M_{1n} = V_{1n}M_n, \quad (17)$$

$$M_{2n} = V_{2n}M_n, \quad (18)$$

$$V_{1n} = \{(-B_{12}b^2 v_n) - (v_n(B_{13}v_n^2 - b^2 - K_1))\}M_n/i\{(-B_{12}bv_n^2) + b((B_{15}v_n^2 - B_{14}b^2 - K_1))\},$$

$$V_{2n} = \{B_9(-v_n H_{1n} + ib)\}M_n/\{(\omega(B_8 - B_{10}\omega)) + B_6(v_n^2 - b^2) + B_7\},$$
$$K_1 = (1 + \varepsilon_0\mu_0^2 H_0^2/\rho)\omega^2, n = 1, 2, 3.$$

The solutions of the total displacement component functions and stresses on the material in the dimensionless form are as follows:

$$u_1 = M_n e^{-v_n x_2 + \omega t + ibx_1}, u_2 = M_n V_{1n} e^{-v_n x_2 + \omega t + ibx_1},$$
$$\phi = M_n V_{2n} e^{-v_n x_2 + \omega t + ibx_1},$$

$$\alpha_{11} = \{ib(1 - (\mu_0 H_0^2/B_1)) - v_n V_{1n}B_{16} + V_{2n}\}M_n e^{-v_n x_2 + \omega t + ibx_1} - P/B_1,$$

$$\alpha_{22} = \{ibB_{16} - v_n V_{1n}B_{17} + V_{2n}\}M_n e^{-v_n x_2 + \omega t + ibx_1} - P/B_1,$$

$$\alpha_{12} = \{ibV_{1n}B_{31} - v_n B_{13}\}M_n e^{-v_n x_2 + \omega t + ibx_1},$$

$$\alpha_{21} = \{ibV_{1n}B_{13} - v_n B_{31}\}M_n e^{-v_n x_2 + \omega t + ibx_1}, n = 1, 2, 3.$$

$$B_{16} = (\lambda + \alpha)/B_1, B_{17} = (\lambda + 2\mu_T)/B_1, B_{31} = (\mu_L + P/2)/B_1.$$

5. Corrugated and Impedance Conditions

The corrugated boundary of the fiber-reinforced half-space with voids is assumed to be denoted by $x_2 = \eta(x_1)$, where $\eta(x_1)$ obeys the trigonometric Fourier series and presented as:

$$\eta(x_1) = \sum_{n=1}^{\infty}(\varsigma_n e^{inbx_1} + \varsigma_{-n}e^{-inbx_1}) \quad (19)$$

Following Asano [5], $\eta(x_1) = a\cos bx_1$, where a is the amplitude of the grooved boundary and b is the wavenumber linked to the grooved boundary surface with the wavelength being $2\pi/b$. Thus, the boundary conditions of the model are as follows:

i. Corrugated and impedance boundary conditions for the initially stressed medium w.r.t x_2 and mechanical force becomes:

$$\alpha_{22} - \eta'(x_1)\alpha_{21} + \bar{\alpha}_{22} + \omega Z_2 u_2 + P = P_1 e^{\omega t + ibx_1},$$
$$\alpha_{12} - \eta'(x_1)\alpha_{11} + \omega Z_1 u_1 + P\varpi_{12} = 0,$$
$$x_2 = \eta(x_1), \text{ for all } x_1 \text{ and } t.$$

ii. Voids and its associated void source boundary conditions become:

$$\xi\phi_{,2} = P_2 e^{\omega t + ibx_1}, \text{ at } x_2 = \eta(x_1), \text{ respectively.}$$

P_1 is the mechanical force and P_2 is the void source parameter. $\bar{\alpha}_{22}$ is an added stress on the material due to Maxwell's theory, Abd-Alla et al. [3] and Anya et al. [9]. The combination of the stresses and the grooved boundary conditions of the porous fiber-reinforced material, tangential, and normal displacement components multiply by the frequency, respectively, the initial stress components and as applications, Ailawalia et al. [25], yields (i) above when subjected to

mechanical force. Z_1 and Z_2 are the impedance parameters. Applying the boundary conditions (i–ii) gives the system of equations below which are non-homogeneous linear equations:

$$\{\{ibB_{16} - \nu_n F_{1n}B_{17} + F_{2n}\} + ab\sin bx_1\{(ibB_{13}F_{1n} - \nu_n B_{31})\}$$
$$+ \{\omega F_{1n}Z_2 + \mu_0 H_0^2(ib - \nu_n F_{1n})\}\}M_n e^{-\nu_n \eta(x_1)}$$
$$= P_1/B_1, \tag{20}$$

$$\{\{ibV_{1n} - \nu_n\}B_{13}^* + ab\sin bx_1\{ib(1 - (\mu_0 H_0^2/B_1)) - \nu_n V_{1n}B_{16}$$
$$+ V_{2n}\} + \{\omega Z_1\}\}M_n e^{-\nu_n \eta(x_1) + \omega t + ibx_1}$$
$$= (abP/B_1)\sin bx_1, \tag{21}$$

$$\{(-\nu_n V_{2n})\}M_n e^{-\nu_n \eta(x_1)} = P_2/B_1. \tag{22}$$

$$B_{13}^* = \mu_L/B_1, \ n = 1, 2, 3.$$

6. Rayleigh Wave

Equations (20–22) yield the solution of the displacement components of the waves and stresses on the material when $M_n, n = 1, 2, 3$ are solved for. If $P_1 = P_2 = P = 0$, the traction-free grooved boundary conditions are recovered. When the mechanical force and void source are removed from the material, the shear stress boundary condition which is in its free boundary state is said to be non-homogeneous due to the initial stress on the material and the choice of the corrugated boundary surfaces. In accordance with this, a novel equation called the dispersion relations for the Rayleigh wave in a porous fiber-reinforced half-space material with grooved and impedance boundary characteristics influenced by magnetic fields is obtained for the model if $P_1 = P_2 = P = 0$, and for a non-trivial solution of the resulting homogeneous system of Equations (20–22), that is $|t_{ij}| = 0$, for the column matrix $|M_i|, \neq 0, i = j = 1, 2, 3$.

7. Computational Results and Discussion

The physical parameters Othman et al. [26] of fiber reinforcements and other constants as given below are used in studying the characteristics of the dispersion relations of the modeled problem as it relates to the effects of magnetic fields, grooved, and impedance boundary exhibitions on the material. These effects are shown in Figures 1–5 and in line with the solutions of the equations of motion and dimensionless boundary conditions contained therein.

$$\mu_L = 2.45 \times 10^9 \, kg \, m^{-1}s^{-2}; \mu_T = 1.89 \times 10^9 kg \, m^{-1}s^{-2};$$
$$\lambda = 9.4 \times 10^9 \, kg \, m^{-1}s^{-2}; \alpha = -1.28 \times 10^9 kg \, m^{-1}s^{-2};$$
$$\beta = 0.32 \times 10^9 \, kg \, m^{-1}s^{-2}; \alpha = -1.28 \times 10^9; a = 0.1; b = 0.3;$$
$$\omega = (-0.3 + i0.1)rad/s; H_0 = 500A/m; t = 0.3s;$$
$$\kappa = 1.753 \times 10^{-15}; P_1 = 0; P_2 = 0; P = 0; \xi = 1.13849 \times 10^{11};$$
$$\xi_1 = 3.668 \times 10^{-4}; \varpi = 0.0787 \times 10^{-2}; Z_1 = 0.5; Z_2 = 0.7.$$
$$\omega_0 = 1.475 \times 10^{12}; \rho = 1.7kg \, m^{-3}.$$

Figure 1 shows the variations occasioned on the dispersion relation $|\nabla| = |t_{ij}|$ of Rayleigh wave versus x_1 coordinate for varying amplitude of the corrugated boundary a, when the impedance $Z_i, i = 1, 2$, wavenumber b, and magnetic fields H_0 parameters are constant on
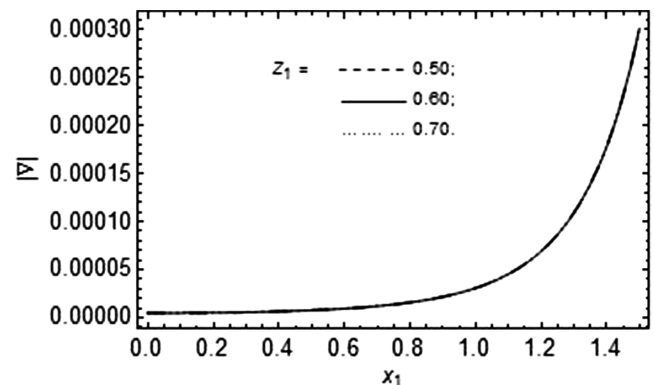

Figure 1
The variations of dispersion relation $|\nabla| = |t_{ij}|$ of Rayleigh wave versus x_1(m) for distinct values of amplitude of grooved boundary a.
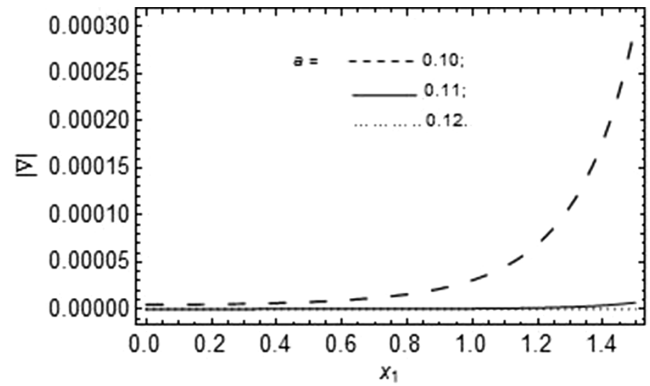
the material while $P_1 = P_2 = P = 0$. Hence, Figure 1 demonstrates that the dispersion relation of the Rayleigh wave attains maximum amplitude near $x_1 = 1.5$., while the minimum distribution profile of the dispersion relation of the Rayleigh waves exists in the range $0 \leq x_2 \leq 1.15$. However, an increase in the amplitude a of the grooved boundary of the material decreases the distribution of the dispersions of the Rayleigh wave. This physically showed that the grooved boundary characteristics of the material will damp the dispersion relations of the Rayleigh wave on the material.

In a similar manner, Figure 2 shows the behavior of the dispersion relation $|\nabla| = |t_{ij}|$ of Rayleigh wave versus x_1 coordinate for varying impedance Z_1 when the magnetic fields H_0, impedance Z_2 and amplitude of the grooved boundary a, and the wave number b are constant on the material while $P_1 = P_2 = P = 0$. The dispersion relation $|\nabla| = |t_{ij}|$ attains maximum amplitude near 1.5. Increasing the impedance Z_1 depicted neither increase nor decrease in the amplitudes of the dispersion profile as it fast attained uniform behavior between $0 \leq x_1 \leq 1.5$, i.e., all through the length of the material. The minimum amplitudes for the profile hold for $0 \leq x_1 < 0.4$. This shows that the impedance Z_1 has demonstrated a mechanical resistance to change for the given dispersion relations which will in turn be characterized by the material.

Figure 2
The variations of dispersion relation $|\nabla| = |t_{ij}|$ of Rayleigh wave versus x_1(m) for distinct values of impedance Z_1.

Consequently, Figure 3 stipulates the effects on dispersion relation $|\nabla| = |t_{ij}|$ of Rayleigh wave versus x_1 coordinates in meters for distinct values of magnetic fields H_0 when the impedance $Z_i, i = 1, 2$ and grooved parameters are constant on the material while $P_1 = P_2 = P = 0$. The dispersion relation at this instance attains its maximum amplitude of distribution near $x_1 = 1.5$. Furthermore, an increase in the magnetic fields H_0 increases the dispersion relations, sequentially. This physically shows that the magnetic field is acting as a push to the dispersion relations of the wave's distributions on the material.

Figure 3

The variations of dispersion relation $|\nabla| = |t_{ij}|$ of Rayleigh wave versus x_1(m) for distinct values of magnetic fields H_0.
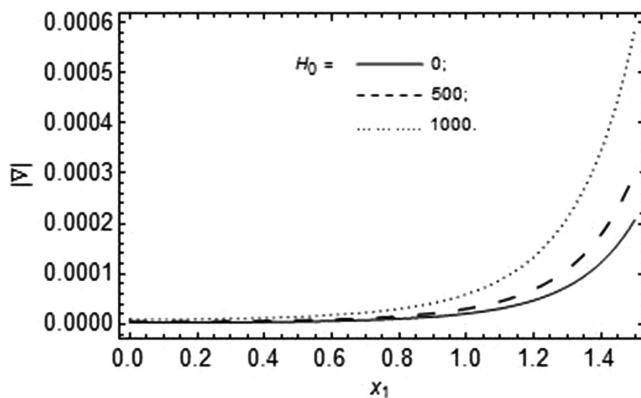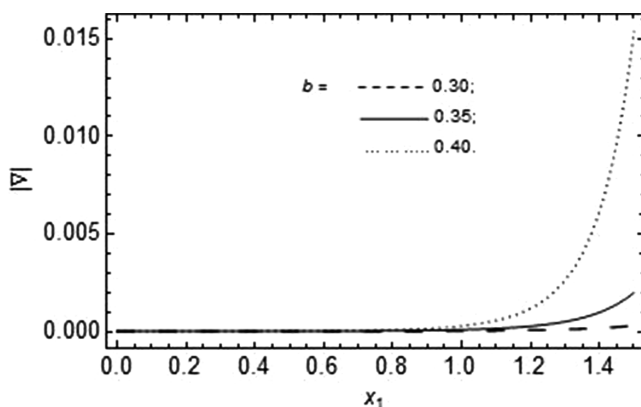

Figure 4 demonstrates the effects on the dispersion relation $|\nabla| = |t_{ij}|$ of Rayleigh wave versus x_1 coordinate for varying wavenumber b which is linked to the grooved boundary when the magnetic fields H_0, impedance $Z_i, i = 1, 2$, and amplitude of the grooved boundary a parameters are constant on the material while $P_1 = P_2 = P = 0$. Thus, it is conspicuous from Figure 4 that the dispersion relation attains maximum distribution in its variation for $x_1 = 1.5$. Uniform behaviors were felt in the range $0 \leq x_1 \leq 0.85$ where the minimum amplitude of the dispersion holds. Be that as it may, increasing the wavenumber b associated with the grooved boundary, increases the dispersion relations of the Rayleigh wave on the material after uniform characteristics were observed in the range $0 \leq x_1 \leq 0.85$.
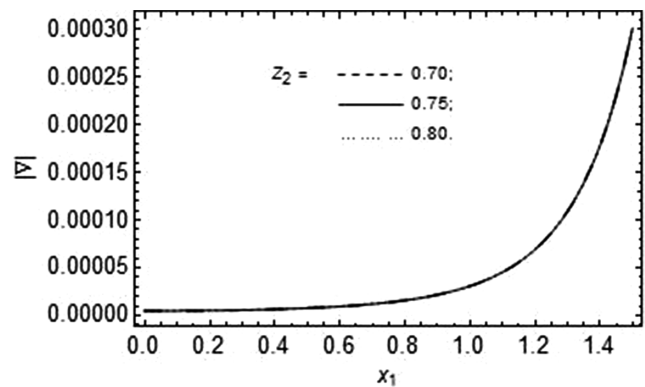
Figure 4

The variations of dispersion relation $|\nabla| = |t_{ij}|$ of Rayleigh wave versus x_1(m) for distinct values of wavenumber b.

Accordingly, Figure 5 depicts the behavior of the dispersion relation $|\nabla| = |t_{ij}|$ of Rayleigh wave versus x_1 coordinate for varying impedance Z_2 when the magnetic fields H_0, impedance Z_1 and amplitude of the grooved boundary a, and the wave number b parameters are constant on the material while $P_1 = P_2 = P = 0$. The dispersion relation $|\nabla| = |t_{ij}|$ attains maximum profile near 1.5. Increasing the impedance Z_2 depicted neither increase nor decrease in the amplitudes of the dispersion profile as it fast attains uniform behavior between $0 \leq x_1 \leq 1.5$. The minimum amplitudes for the respective distributions hold for $0 \leq x_1 < 0.4$. This shows that the impedance Z_2 has demonstrated a mechanical-like resistance to change for the given dispersion relations which will in turn be exhibited by the material.
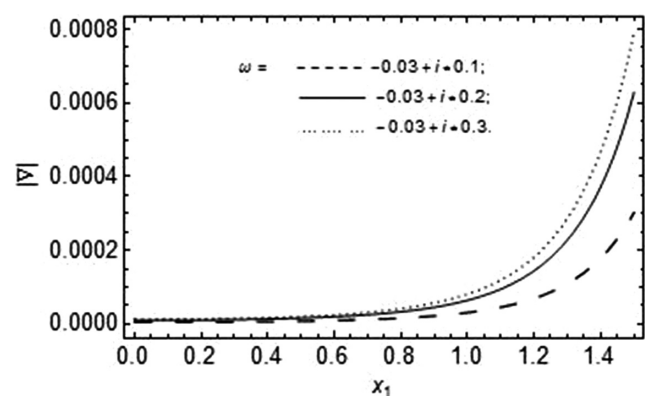
Figure 5

The variations of dispersion relation $|\nabla| = |t_{ij}|$ of Rayleigh wave versus x_1(m) for distinct values of impedance Z_2.

Furthermore, Figure 6 stipulates the behavior of the dispersion relation $|\nabla| = |t_{ij}|$ of Rayleigh wave versus x_1 coordinate for varying phase velocity ω of the wave when the magnetic fields H_0, impedances Z_1, Z_2, amplitude of the grooved boundary a, and the wave number b parameters are constant on the material where $P_1 = P_2 = P = 0$. We deduce that an increase in the phase velocity ω of the wave depicts a corresponding increase in the amplitudes of the dispersion profile of the Rayleigh wave and vice versa on the material along $0 < x_1 \leq 1.5$.

Figure 6

The variations of dispersion relation $|\nabla| = |t_{ij}|$ of Rayleigh wave versus x_1(m) for distinct values of phase velocity ω

Subsequently, Figure 7(a–d) showcases the effects on the dispersion relation $|\nabla| = |t_{ij}|$ of Rayleigh wave versus x_1 coordinate for varying void parameters $\omega_0; \xi_1; \kappa; \varpi$, when the magnetic fields H_0,

Figure 7
The variations of dispersion relation $|\nabla| = |t_{ij}|$ of Rayleigh wave versus x_1(m) for distinct values of void parameters $\omega_0; \xi_1; \kappa; \varpi$.
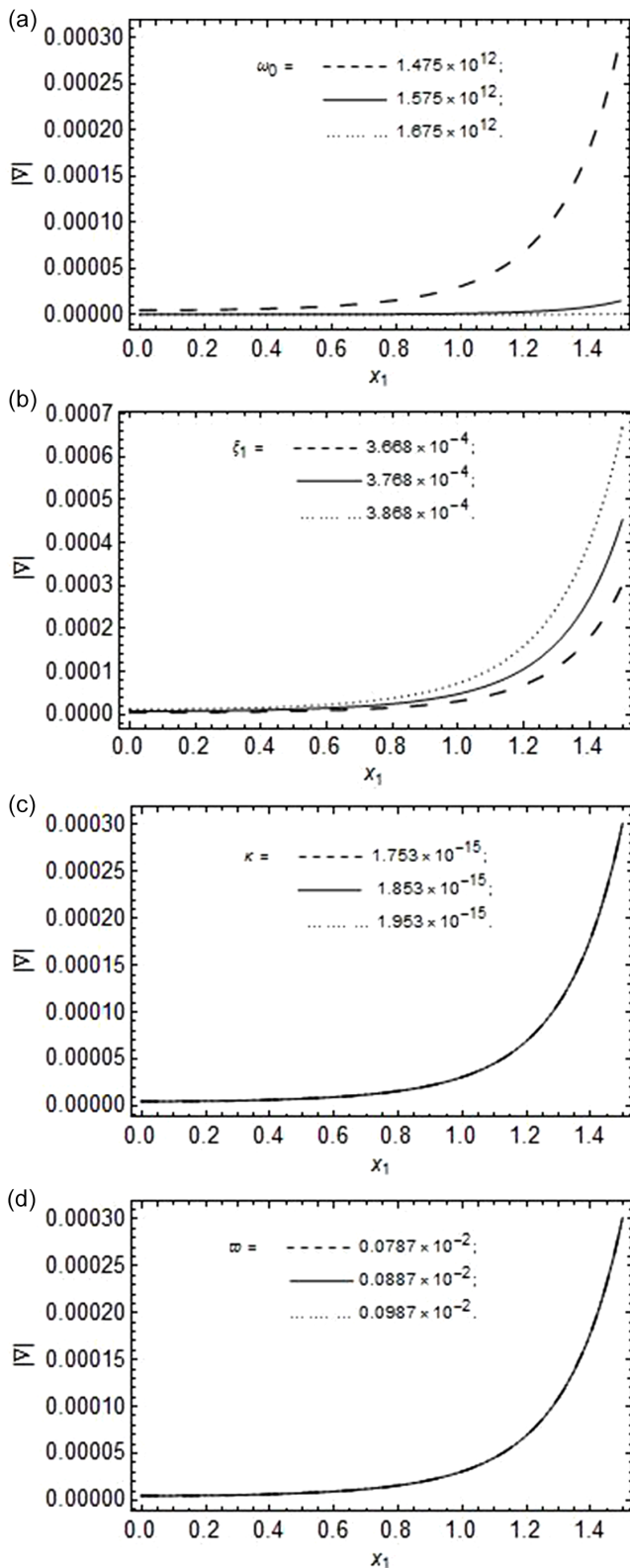
impedance $Z_i, i = 1, 2$, and grooved parameters a, b are constant on the material such that $P_1 = P_2 = P = 0$. An increase in the void parameter ω_0 leads to a simultaneous decrease on the Rayleigh wave distribution on the material while the void parameter ξ_1 tends to increase the distribution of the Rayleigh wave profile on the material for increased values. Both void parameters κ and ϖ maintained uniform behaviors for the chosen values of the respective varying void parameters, that is, increase in the void parameters ϖ and κ depicts neither increase nor decrease of the Rayleigh wave distribution, especially at this given values.

8. Conclusion

A novel model to investigate elastic surface waves and analyze the dispersion relation of Rayleigh-type wave on a magneto-elastic material with corrugated and impedance boundaries possessing initial stress and voids was carried out. The solutions of the displacement and stress components on the material were developed, and it showed that they depend on all the considered physical quantities. Sequel to this, observations were made on the contributing physical constants or fields on the material such that Rayleigh waves became visibly possible for the choice or nature of the boundary surface of the material only if $P_1 = P_2 = P = 0$, i.e., Mechanical force, void source, and initial stress are negligible. Furthermore, an increase in the amplitude of the corrugated boundary surface decreases the dispersion relations of the Rayleigh wave. Also, increasing the wavenumber associated with the corrugated boundary increases the dispersion relations of the Rayleigh wave while noting some uniform behaviors. The magnetic fields increase the dispersion relation of the Rayleigh wave profiles on the material, whereas the impedances Z_1 and Z_2 depicted neither increase nor decrease in the profile of the dispersion relation for the respective chosen values as observed at these points. This shows that the impedances acted as a mechanical resistance to the dispersion relations of the Rayleigh wave at every point on the material, especially for the chosen values. Subsequently, it is noted that the dispersion relations of the wave increase for increasing phase velocity and some parameters of voids. Also, a void parameter could trigger a decrease on the distribution profile of the dispersion relations of the Rayleigh wave when increased while noting some uniform exhibitions from the other varying void parameters.

Recommendations

The authors are recommending some future works and deductions on the attenuation and velocities associated with Rayleigh wave propagation on the material as regards the considered model. Thus, this study would be helpful in the fields where Mathematics of waves, stress-strain fiber analysis, geophysics, civil and structural engineering analysis, among others are paramount.

Ethical Statement

This study does not contain any studies with human or animal subjects performed by any of the authors.

Conflicts of Interest

The authors declare that they have no conflicts of interest to this work.

Data Availability Statement

Data sharing is not applicable to this article as no new data were created or analyzed in this study.

Author Contribution Statement

Augustine Igwebuike Anya: Conceptualization, Methodology, Software, Validation, Formal analysis, Investigation, Resources, Data curation, Writing – original draft, Writing – review & editing, Visualization, Supervision, Project administration. **Ugochukwu David Uche:** Methodology, Software, Validation, Formal analysis, Investigation, Resources, Writing – original draft, Writing – review & editing, Visualization. **Christian Nwachioma:** Methodology, Software, Validation, Investigation, Resources, Writing – original draft, Writing – review & editing, Visualization.

References

[1] Spencer, A. J. M. (1972). *Deformations of fibre-reinforced materials*. UK: Oxford University Press.

[2] Biot, M. A. (1965). *Mechanics of incremental deformations*. USA: John Wiley and Sons, Inc.

[3] Abd-Alla, A. M., Abo-Dahab, S. M., & Khan, A. (2017). Rotational effects on magneto- thermoelastic stonely, Love, and Rayleigh waves in fibre-reinforced anisotropic general viscoelastic media of higher order. *CMC*, *53*, 49–72.

[4] Cowin, S. C., & Nunziato, J. W. (1983). Linear elastic materials with voids. *Journal of Elasticity*, *13*(2), 25–147.

[5] Asano, S. (1966). Reflection and refraction of eastic waves at a corrugated interface. *Bulletin of the Seismological Society of America*, *56*(1), 201–221.

[6] Singh, B. (2017). Reflection of elastic waves from plane surface of a half-space with impedance boundary conditions. *Geoscience Research*, *2*(4), 242–253.

[7] Abd-Alla, A. M., Abo-Dahab, S. M., & Alotaibi, A. H. (2016). Effect of the rotation on a non-homogeneous infinite elastic cylinder of orthotropic material with magnetic field. *Journal of Computational and Theoretical Nanoscience*, *13*(7), 4476–4492.

[8] Anya, A. I., & Khan, A. (2020). Reflection and propagation of magneto-thermoelastic plane waves at free surfaces of a rotating micropolar fibre-reinforced medium under G-L theory. *International Journal of Acoustics & Vibration*, *25*(2), 190–199.

[9] Anya, A. I., Akhtar, M. W., Abo-Dahab, M. S., Kaneez, H., Khan, A., & Jahangir, A. (2018). Effects of a magnetic field and initial stress on reflection of SV-waves at a free surface with voids under gravity. *Journal of the Mechanical Behaviour of Materials*, *27*, 5–6.

[10] Chattopadhyay, A. (1975). On the dispersion equation for Love wave due to irregularity in the thickness of non-homogeneous crustal layer. *Acta Geophysica Polonica*, *23*, 307–317.

[11] Das, S. C., Acharya, D. P., & Sengupta, D. R. (1992). Surface waves in an inhomogeneous elastic medium under the influence of gravity. *Revue roumaine des sciences techniques. Série de mécanique appliquée*, *37*, 539–551.

[12] Dey, S., & Addy, S. K. (1977). Reflection of plane waves under initial stress at a free surface. *International Journal of Nonlinear Mechanics*, *12*(6), 372–381.

[13] Gupta, R. R. (2014). Surface wave characteristics in amicropolar transversely isotropic half-space underlying an inviscid liquid layer. *International Journal of Applied Mechanics and Engineering*, *19*(1), 49–60.

[14] Nunziato, J. W., & Cowin, S. C. (1979). A nonlinear theory of elastic materials with voids. *Archives for Rational Mechanics and Analysis*, *72*(2), 175–201.

[15] Puri, P., & Cowin, S. C. (1985). Plane waves in linear elastic materials with voids. *Journal of Elasticity*, *15*(2), 167–183.

[16] Munish, S., & Sharma, A. (2016). Propagation of SH waves in a double non-homogeneous crustal layers of finite depth lying over an homogeneous half-space. *Latin American Journal of Solids & Structures*, *13*(14), 2628–2642.

[17] Roy, I., Acharya, D. P., & Acharya, S. (2018). Propagation and reflection of plane waves in a rotating magneto-elastic fibre-reinforced semi space with surface stress. *Mechanics and Mechanical Engineering*, *22*(4), 939–957.

[18] Singh, S. S., & Tomar, S. K. (2008). qP-wave at a corrugated interface between two dissimilar pre-stressed elastic half-spaces. *Journal of Sound and Vibration*, *317*(3), 687–708.

[19] Singh, D., & Sindhu, R. (2011). Propagation of waves at interface between a liquid half- space and an orthotropic micropolar solid half-space. *Advances in Acoustics and Vibration*, *2011*, 1–5.

[20] Singh, A. K., Das, A., Kumar, S., & Chattopadhyay, A. (2015). Influence of corrugated boundary surfaces, reinforcement, hydrostatic stress, heterogeneity and anisotropy on Love-type wave propagation. *Meccanica*, *50*(12), 2977–2994.

[21] Singh, A. K., Mistri, K. C., & Pal, M. K. (2018). Effect of loose bonding and corrugated boundary surface on propagation of Rayleigh-type wave. *Latin American Journal of Solids and Structures*, *15*(1), e01.

[22] Sunita, D., Suresh, K. S., & Kapil, K. K. (2019). Reflection at the free surface of fibre-reinforced thermoelastic rotating medium with two temperature and phase- lag. *Applied Mathematical Modelling*, *65*, 106–119.

[23] Zghal, S., Ataoui, D., & Dammak, F. (2021). Free vibration analysis of porous beams with gradually varying mechanical properties. *Proceedings of the Institution of Mechanical Engineers, Part M: Journal of Engineering for the Maritime Environment*, *236*(3), 800–812.

[24] Kundu, S., Maity, M., Pandit, D. K., & Gupta, S. (2019). Effect of initial stress on the propagation and attenuation characteristics of Rayleigh waves. *Acta Mechanica*, *230*(1), 67–85.

[25] Ailawalia, P., Sachdeva, S. K., & Pathania, D. (2015). A two dimensional fibre reinforced micropolar thermoelastic problem for a half-space subjected to mechanical force. *Theoretical and Applied Mechanics*, *42*(1), 11–25.

[26] Othman, M. I. A., Lotfy, K., Said, S. M., & Bég, O. A. (2012). Wave propagation in a fiber-reinforced micropolar thermoelastic medium with voids using three models. *International Journal of Applied Mathematics and Mechanics*, *8*(12), 52–69.

Appendix

$G_1 = B_6 B_{13} B_{15};$

$G_2 = \left\{ \left(\rho B_{13}(B_{11}B_9 - (B_7 + \omega(B_8 - \omega B_{10}))B_{15}) - B_6 \left(b^2 i^2 \rho B_{12}^2 + B_{15}(\rho(b^2 + \omega^2) + \omega^2 H_0^2 \varepsilon_0 \mu_0^2) + B_{13} \begin{pmatrix} b^2 \rho B_{14} + b^2 \rho B_{15} \\ + \omega^2(\rho + H_0^2 \mu_0^2) \end{pmatrix} \right) \right) \right\} / \rho;$

$G_3 = \dfrac{1}{\rho^2} \left(B_6(b^4 i^2 \rho^2 B_{12}^2 + b^2 \rho B_{13}(b^2 \rho B_{14} + \omega^2(\rho + H_0^2 \mu_0^2)) + (\rho(b^2 + \omega^2) + \omega^2 H_0^2 \varepsilon_0 \mu_0^2) \begin{pmatrix} b^2 \rho B_{14} + \\ b^2 \rho B_{15} + \omega^2 \begin{pmatrix} \rho + \\ H_0^2 \mu_0^2 \end{pmatrix} \end{pmatrix} \right) \right.$

$\qquad + \rho \left(-B_{11}B_9(b^2 \rho + \rho \omega^2 + 2b^2 i^2 \rho B_{12} - b^2 i^2 \rho B_{15} + \omega^2 H_0^2 \varepsilon_0 \mu_0^2) + (B_7 + \omega(B_8 - \omega B_{10})) \left(b^2 i^2 \rho B_{12}^2 + B_{15}(\rho(b^2 + \omega^2) + \omega^2 H_0^2 \varepsilon_0 \mu_0^2) \right. \right.$

$\qquad \left. \left. \left. + B_{13} \begin{pmatrix} b^2 \rho B_{14} + \omega^2 \\ (\rho + H_0^2 \mu_0^2) \end{pmatrix} \right) \right) \right);$

$G_4 = -\left\{ \left(b^2 \rho B_{14} + \omega^2 \begin{pmatrix} \rho + \\ H_0^2 \mu_0^2 \end{pmatrix} \right) (b^2 \rho \omega B_8 + \rho \omega^3 B_8 + b^2 B_{11} i^2 \rho B_9 - b^2 \rho \omega^2 B_{10} - \rho \omega^4 B_{10} + \omega^3 B_8 H_0^2 \varepsilon_0 \mu_0^2 - \omega^4 B_{10} H_0^2 \varepsilon_0 \mu_0^2 \right.$

$\qquad \left. + b^2 B_6(\rho(b^2 + \omega^2) + \omega^2 H_0^2 \varepsilon_0 \mu_0^2) + B_7(\rho(b^2 + \omega^2) + \omega^2 H_0^2 \varepsilon_0 \mu_0^2)) \right\} / \rho^2.$